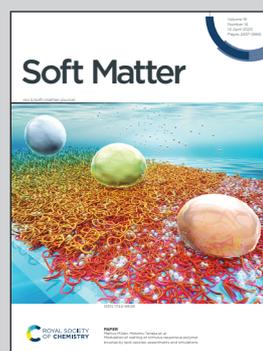**Highlighting research from Prof. Takashi Miyata's laboratory at Kansai University, Osaka, Japan.**

Relatively homogeneous network structures of temperature-responsive gels synthesized *via* atom transfer radical polymerization

Dynamic light scattering measurements reveal that ATRP suppresses the inhomogeneity of temperature-responsive networks effectively. Quantitative evaluations of the inhomogeneity by the standard deviation of the scattered intensity are useful in the investigation of the structure–property relationships of temperature-responsive gels.

As featured in:

See Takashi Miyata *et al.*,
Soft Matter, 2023, **19**, 2505.

ROYAL SOCIETY
OF **CHEMISTRY**

rsc.li/soft-matter-journal

Soft Matter

Check for updates

Relatively homogeneous network structures of temperature-responsive gels synthesized *via* atom transfer radical polymerization†

Chisa Norioka,[a] Akifumi Kawamura [ID] [ab] and Takashi Miyata [ID] ⋆[ab]

The network structures of poly(*N*-isopropylacrylamide) (PNIPAAm) gels prepared by atom transfer radical polymerization (ATRP) were compared with those prepared by free radical polymerization (FRP), as a conventional radical polymerization. Temperature-responsive shrinkage was observed in the PNIPAAm gels prepared by ATRP and FRP (ATRP and FRP gels), which depended on the cross-linker content. From the light-scattered intensities, $\langle I \rangle_T$, measured at the different sample positions, we used the partial heterodyne method to determine the dynamic fluctuation, $\langle I \rangle_F$, spatial component, $\langle I \rangle_C$, and correlation length, ξ, of the ATRP and FRP gels, as a function of the cross-linker content and temperature. While there is little difference in $\langle I \rangle_F$ and ξ between the ATRP and FRP gels, $\langle I \rangle_C$ of the ATRP gel was smaller than that of the FRP gel. In addition, we calculated the standard deviation of $\langle I \rangle_T$ for the ATRP and FRP gels, as a function of temperature to quantify the inhomogeneity of the gel networks. The standard deviation revealed that increasing cross-linker content and temperature makes the gel networks more inhomogeneous. The dynamic light scattering (DLS) measurement used to characterize the gel network revealed that ATRP suppresses inhomogeneity more effectively than FRP. The standard deviation of the scattered intensity is used in this study to quantify the inhomogeneity of the network structures. Quantitative evaluations of the inhomogeneity of the network structures by the standard deviation of the scattered intensity are useful in the investigation of the structure−property relationships of gels.

Introduction

Polymer gels with three-dimensional (3D) networks of hydrophilic polymers have high water absorption and are highly swollen in aqueous media. Some polymer gels exhibit a drastic change in volume in response to external stimuli, such as pH, temperature, electrical field, and target molecules.[1–14] Such gels, known as stimuli-responsive gels, have been developed as smart soft materials for drug delivery systems, sensors, actuators, and so on. The properties and functions of polymer gels directly depend on their network structure. For example, well-designed network structures, such as slide-ring-cross-linked networks,[15,16] nanocomposite structures using inorganic nanoclays as cross-linkers,[17] double networks with sacrificial bonds,[18–20] and networks with a lot of polymer chain entanglements,[21] significantly improve the mechanical

properties of polymer gels. Polymer gels with well-designed structures demonstrate high tensile strength and mechanical toughness. The network structures of stimuli-responsive gels also influence their responsiveness. The formation of heterogeneous domains results in the formation of rapidly stimuli-responsive gels.[22–25] These results show that designs and characterizations of the network structure of polymer gels are critical in understanding the properties and functions of polymer gels. In addition, well-designed polymer networks result in unique properties and functions.

Generally, the cross-linking density from the swelling degree and compression modulus is used to indirectly evaluate the network structures of polymer gels. Scattering methods, such as small-angle X-ray (SAXS), neutron scattering (SANS), and dynamic light scattering (DLS) are also powerful tools for analyzing the network structures of polymer gels.[26] For example, the network structures of tough gels, such as slide-ring-cross-linked, nanocomposite, and double network gels have been investigated using the scattering method.[27,28] Their investigations revealed that the excellent mechanical properties of tough gels are attributed to their distinctive network structures. Furthermore, four-armed poly(ethylene glycol) (Tetra-PEG) gels had homogeneous networks with no defects, as characterized by

[a] *Department of Chemistry and Materials Engineering, Kansai University, 3-3-35, Yamate-cho, Suita, Osaka 564-8680, Japan. E-mail: tmiyata@kansai-u.ac.jp*
[b] *Organization for Research and Development of Innovative Science and Technology, Kansai University, 3-3-35, Yamate-cho, Suita, Osaka 564-8680, Japan*

† Electronic supplementary information (ESI) available: details of decomposition plots and a histogram of light scattered intensity. See DOI: https://doi.org/10.1039/d3sm00044c

a light scattering method.[29] The high mechanical properties of Tetra-PEG gels indicate that their network is closer to an ideal polymer network than any other conventional model network.[30] The homogeneity of Tetra-PEG gel networks can be controlled by modulating the length of the polymer chain and the concentration during polymerization.[31,32,34–37]

In the DLS measurements, temporal fluctuations are usually analyzed using the intensity or the correlation function. Unlike the DLS measurements of dynamic polymer and colloidal solutions, those of polymer gels provide speckle patterns in the scattered intensity, depending on the sample position.[33–35] While the scattered intensity of general polymer solutions is not spatially dependent, that of polymer gels is. The ensemble average of the scattered intensity for polymer gels is not equal to its time average because of frozen fluctuations due to cross-linking. Therefore, the scattered intensity ($\langle I \rangle_T$) of the polymer gels is composed of two contributions, such as the dynamic and static fluctuations, as represented by eqn (1).[26,34–40]

$$\langle I \rangle_T = \langle I \rangle_F + \langle I \rangle_C \qquad (1)$$

where $\langle I \rangle_F$ is the dynamic concentration fluctuations and $\langle I \rangle_C$ is the static component with spatial dependence derived from cross-linking. The correlation function for polymer solutions is given by a single exponential function in the DLS measurements[37] but that of polymer gels is not given because of the spatial inhomogeneity. In the past, heterodyne-type analysis was often used to characterize the network structures of polymer gels.[41,42] Pusey and van Megen reported the partial heterodyne method as a different method for the nonergodic medium.[33] Shibayama et al. characterized the network structures of poly(N-isopropylacrylamide) (PNIPAAm) gels, representing temperature-responsive gels, using the partial heterodyne method.[34–40] Their previous studies demonstrate that DLS measurements and partial heterodyne methods are useful in characterizing the network structure of polymer gels.

In a previous study, we synthesized PNIPAAm gels using atom transfer radical polymerization (ATRP), which is a controlled radical polymerization (CRP). The temperature-responsiveness and mechanical properties of PNIPAAm gels synthesized via ATRP differ from those synthesized via free radical polymerization (FRP).[43] Recently, a few researchers prepared PNIPAAm gels using reversible addition–fragmentation chain transfer (RAFT) polymerization, another CRP, and investigated the temperature-responsiveness of the resulting gels.[44,45] Such a few studies revealed that there are significant differences in the temperature-responsiveness and mechanical properties between PNIPAAm gels synthesized via CRP and FRP. The differences between the PNIPAAm gels synthesized via CRP and FRP may be explained by the inhomogeneity of their gel networks. However, to the best of our knowledge, no report compares the inhomogeneity of networks between PNIPAAm gels synthesized via CRP and FRP by quantitative characterizations of their networks using DLS measurements. In this study, we used DLS measurements to characterize the network structures of PNIPAAm gels synthesized via ATRP and FRP. The inhomogeneity of the networks formed via ATRP was quantitatively compared with that via FRP between the PNIPAAm gels from the dynamic and static fluctuations contributing to the light-scattered intensity of the PNIPAAm gels. This study also proposes a quantitative evaluation of the inhomogeneity of the networks using the standard deviation of the scattered intensity depending on the sample positions. This is the first paper proposing a quantitative evaluation of the inhomogeneity of the network structures by the standard deviation of the scattered intensity although there are some reports on responsive behaviors of temperature-responsive gels synthesized via controlled radical polymerization such as ATRP and RAFT polymerization.

Experimental

Materials

N-Isopropylacrylamide (NIPAAm), N,N′-methylenebisacrylamide (MBAA), N,N,N′,N′-tetramethyl ethylenediamine (TEMED), ammonium persulfate (APS), copper(ii) chloride and ascorbic acid were purchased from Wako Pure Chemical Industries (Wako, Japan). 2-Chloropropionamide (2-Cl-PA) was purchased from Sigma-Aldrich (Tokyo, Japan). Tris[2-(dimethylamino)-ethyl]amine (Me$_6$T-REN) was purchased from Alfa Aesar (Ward Hill, MA).

Synthesis of PNIPAAm gels by ATRP

The PNIPAAm gels were prepared by copolymerization of NIPAAm and MBAA via ATRP in glass molds. The feed compositions for the preparation of the gels are summarized in Table S1 (ESI†). First, NIPAAm (2264 mg, 20.0 mmol), which had been recrystallized from benzene/hexane before use, 2-Cl-PA (5.42 mg, 0.05 mmol), copper(ii) chloride (5.4 mg, 0.04 mmol), and Me$_6$T-REN (12.5 mg, 0.054 mmol) were dissolved in deionized water (10 mL) to prepare an aqueous NIPAAm solution for ATRP. MBAA (45.44 mg, 0.29 mmol), a cross-linker, and ascorbic acid (34.23 mg, 0.19 mmol) were dissolved in deionized water (2 mL) separately. The resulting aqueous MBAA solution was added to the NIPAAm solution (2 mL) to achieve a total volume of 2.9 mL. The resulting monomer mixture and the aqueous ascorbic acid solution were degassed and purged with Ar via freeze–pump–thaw cycles. Then, the aqueous ascorbic acid solution (0.1 mL) was added to the monomer mixture (2.9 mL) with a syringe under Ar and positive pressure before polymerization was started at 5 °C. The reaction mixtures were exposed to an ambient atmosphere to quench the polymerization after 22 h. The resulting PNIPAAm gels were washed by immersion in water for 2 weeks to remove unreacted monomers and initiators.

Synthesis of PNIPAAm gels by FRP

The PNIPAAm gels were prepared by copolymerization of NIPAAm and MBAA via FRP in glass molds. The feed compositions for the preparation of the gels are summarized in Table S2 (ESI†). To prepare an aqueous NIPAAm solution for FRP, NIPAAm, which had been recrystallized from benzene/hexane before use, and TEMED were dissolved in deionized water. MBAA (2264 mg, 20 mmol) and APS (45.21 mg, 0.19 mol) were separately dissolved in 10 and 2 mL of deionized water, respectively. The aqueous MBAA solution was added to the

aqueous monomer solution to achieve a total volume of 2.9 mL. The resulting monomer mixture and aqueous APS solution were degassed and purged with Ar *via* freeze–pump–thaw cycles. After the aqueous APS solution (2.26 mg, 0.01 mol) was added to the mixture, polymerization was started at 5 °C. The reaction mixtures were exposed to an ambient atmosphere to quench the polymerization after 22 h. The resulting PNIPAAm gels were washed by immersion in water for 2 weeks to remove unreacted monomers and initiators.

Water content measurements

The PNIPAAm gels synthesized *via* ATRP and FRP were immersed in water at various temperatures until equilibrium was reached. After the surface water of the swollen gel was removed by lightly blotting with a laboratory tissue, the gel was weighed ($W_{\text{swollen gel}}$). The gels were weighed ($W_{\text{dried gel}}$) after they were dried at 70 °C in an oven for two days. The equilibrium water content of the PNIPAAm gels at various temperatures was determined from the weight of the swollen gel ($W_{\text{swollen gel}}$) and dried gel ($W_{\text{dried gel}}$) using eqn (2).

$$\text{Water content (\%)} = \frac{W_{\text{swollen gel}} - W_{\text{dried gel}}}{W_{\text{swollen gel}}} \times 100 \qquad (2)$$

Compression measurements

The PNIPAAm gels synthesized *via* ATRP and FRP were swollen to equilibrium in water at 25 °C. After the as-prepared and swollen gels were cut to a rectangular shape (width 4 mm, depth 4 mm, height 3.5 mm), their compression tests were performed using a compression velocity of 10 mm min^{-1} and a mechanical testing instrument (SMT1-2-N, Shimadzu Co. Ltd, Kyoto). The compression modulus of the gels was determined from the strain–stress curves obtained during the compression tests using eqn (3).[4,21,46,47]

$$\sigma = G(\alpha - \sigma^{-2}) \qquad (3)$$

where σ is the compression stress, G is the compression modulus, and α is the ratio of the gel thickness before and after the compression. A plot of σ *vs.* $(\alpha - \alpha^{-2})$ showed a linear relationship. The G value is determined using the slope of the linear relationship. Then, the effective cross-linking density, ν_{e}, of the gel was determined using eqn (4)

$$G \approx RT\nu_{\text{e}}\phi^{1/3} \qquad (4)$$

where R is the gas constant, T is the absolute temperature (K), and ϕ is the polymer volume fraction of the as-prepared gel or swollen gel.

Dynamic light scattering (DLS) measurements

The ATRP gels for the DLS measurements were prepared in a DLS sample tube as follows. NIPAAm, 2-Cl-PA, copper(II) chloride, and Me$_6$TREN were dissolved in deionized water to prepare an aqueous NIPAAm solution. MBAA and ascorbic acid were dissolved in deionized water separately. The resulting aqueous MBAA solution was added to the aqueous NIPAAm solution. The resulting mixture was placed in a DLS sample tube fitted

with a rubber septum and degassed using Ar bubbling. The aqueous ascorbic acid solution was degassed using freeze–pump–thaw cycles and purged with Ar. Polymerization was started at 5 °C after the aqueous ascorbic acid solution was added to the DLS sample tube *via* a syringe. The reaction mixtures were exposed to an ambient atmosphere to quench the polymerization after 22 h.

[NIPAAm] : [2-Cl-PA] : [CuCl$_2$] : [Me$_6$TREN] : [ascorbic acid] = 1.33 M : 3.3 × 10^{-3} M : 2.7 × 10^{-3} M : 3.6 × 10^{-3} M : 3.2 × 10^{-3} M. [MBAA] = 1.3 × 10^{-2} M (1 mol%), 4.0 × 10^{-2} M (3 mol%), 6.7 × 10^{-2} M (5 mol%).

The FRP gels for the DLS measurements were prepared in a DLS sample tube as follows. NIPAAm and TEMED were dissolved in deionized water to prepare an aqueous NIPAAm solution. MBAA and APS were dissolved in deionized water. The aqueous MBAA solution was added to the aqueous NIPAAm solution. The resulting mixture was degassed by Ar bubbling in a DLS sample tube fitted with a rubber septum. The mixture and the aqueous APS solution were degassed and purged with Ar using freeze–pump–thaw cycles. Polymerization was started at 5 °C after the aqueous APS solution was added to the DLS sample tube *via* a syringe. The reaction mixtures were exposed to an ambient atmosphere to quench the polymerization.

[NIPAAm] : [TEMED] : [APS] = 1.33 M : 2.6 × 10^{-2} M : 4.9 × 10^{-3} M : 3.6 × 10^{-3} M : 3.3 × 10^{-3} M. [MBAA] = 1.3 × 10^{-2} M (1 mol%), 4.3 × 10^{-2} M (3 mol%), 7.0 × 10^{-2} M (5 mol%).

A dynamic light scattering spectrophotometer (DLS-8000, Otsuka Electronics Co., Ltd, Kyoto) was used for the DLS experiments. The scattering angle was fixed at 60°, and the measurement temperatures were 15 °C, 25 °C, and 30 °C. The partial heterodyne method[34–40] was used to analyze the DLS measurements of the ATRP and FRP gels. The total scattered intensity, $\langle I \rangle_{\text{T}}$, of a polymer gel, is the sum of the dynamic fluctuation, $\langle I \rangle_{\text{F}}$, and the static component derived from spatial fluctuation, $\langle I \rangle_{\text{C}}$ (eqn (1)), as stated in the introduction. The intensity time correlation function, $g^{(2)}(\tau)$, for a gel is determined using eqn (5).

$$g^{(2)}(\tau) = \sigma_{\text{I}}^2 \exp[-2D_{\text{A}}q^2\tau] + 1 \qquad (5)$$

where D_{A} is the apparent diffusion coefficient, q is the magnitude of the scattering vector, and σ_{I}^2 is the initial amplitude of $g^{(2)}(\tau)$. In standard gels, D_{A} and σ_{I}^2 depend on sample position. Specifically, $g^{(2)}(\tau)$ is represented by eqn (6).

$$g^{(2)}(\tau) = X_{\text{P}}^2 \exp(-2Dq^2\tau) + 2X_{\text{P}}(1 - X_{\text{P}}) \times \exp(-Dq^2\tau) + 1 \qquad (6)$$

where D is the collective diffusion coefficient, X_{P} is the ratio of intensity from dynamic fluctuations to that from the total intensity at each sample position (eqn (7)).

$$X_{\text{P}} = \langle I \rangle_{\text{F}} / \langle I \rangle_{\text{T}} \qquad (7)$$

As D and $\langle I \rangle_{\text{F}}$ have the relationship shown in eqn (8),[48] we can determine them by plotting $\langle I \rangle_{\text{T}}/D_{\text{A}}$ *vs.* $\langle I \rangle_{\text{T}}$ based on eqn (9).[34,35]

$$D_{\text{A}} = \frac{D}{2 - X_{\text{P}}} = \frac{D}{2 - \langle I \rangle_{\text{F}} / \langle I \rangle_{\text{T}}} \qquad (8)$$

View Article Online

$$\frac{\langle I\rangle_{\mathrm{T}}}{D_{\mathrm{A}}} = \frac{2}{D}\langle I\rangle_{\mathrm{T}} - \frac{\langle I\rangle_{\mathrm{F}}}{D} \tag{9}$$

D represents the collective diffusion constant of the polymer chains and cross-links in a gel. Furthermore, $\langle I\rangle_{\mathrm{C}}$ can be determined using $\langle I\rangle_{\mathrm{T}}$ and $\langle I\rangle_{\mathrm{F}}$ from eqn (1). In addition, the correlation length, ξ, is related to D using eqn (10).

$$D \cong \frac{kT}{6\pi\eta\xi} \tag{10}$$

where k is the Boltzmann constant, T is the absolute temperature, and η is the viscosity of the solvent. Thus, we determined $\langle I\rangle_{\mathrm{F}}$, $\langle I\rangle_{\mathrm{C}}$, and ξ using eqn (1), (9) and (10) to evaluate the inhomogeneity of the PNIPAAm gels synthesized via ATRP and FRP. In general, it is difficult to perform the DLS measurements of turbid gels. Unfortunately, the gels with a cross-linker content of more than 5 mol% were turbid. Even if the gels were prepared with a cross-linker content of less than 5 mol%, they became turbid at a temperature above the LCST of PNIPAAm. Therefore, in this study, we characterized the network structures of gels with a cross-linker content of 5 mol% or less at a temperature below the LCST of PNIPAAm by the DLS measurements.

Results and discussion

Preparation of PNIPAAm gels by ATRP

In this study, we prepared PNIPAAm gels using two different methods, referred to as ATRP and FRP gels, respectively. We performed the compression tests of their gels to determine their compression modulus (Table S3, ESI†). The cross-linking densities of the as-prepared and swollen ATRP and FRP gels were determined using their compression modulus and swelling ratio (Fig. 1). The cross-linking density is the number of cross-links per polymer volume fraction with the consideration of the swelling ratio. If the number of cross-links in the networks of the as-prepared gel does not change at all during its swelling in aqueous media, the cross-linking density of the as-prepared gel will be the same as that of the swollen gel. Both as-prepared and swollen ATRP gels demonstrated a monotonous increase in crosslinking density with increasing cross-linker content. However, the cross-linking density of both as-prepared and
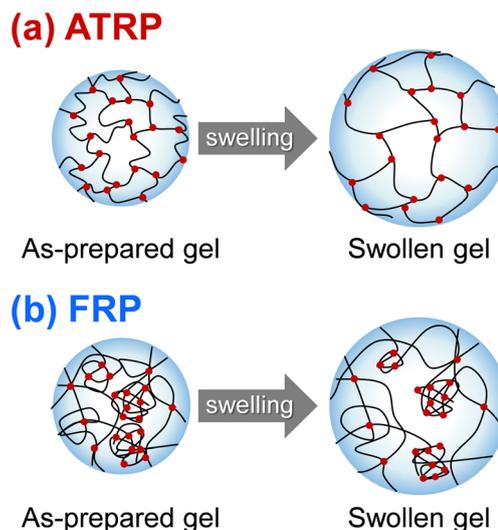

Fig. 2 An illustration of the swelling network structure formed by ATRP (a) and FRP (b).

swollen FRP gels increased gradually with increasing cross-linker content up to 5 mol%, and became almost constant with a cross-linker content of more than 5 mol%. These indicate that most cross-linker MBAA acted as cross-links in the ATRP networks of NIPAAm and MBAA, but some MBAAs did not function as the cross-links in the FRP networks with cross-linker content of more than 5 mol%. Notably, the cross-linking density of the swollen ATRP gel was almost the same as that of the as-prepared ATRP gel although that of swollen FRP gel was lower than that of the as-prepared FRP gel. FRP networks have inhomogeneous structures with many dangling chains, looped chains, and entanglements; thus, their swelling in aqueous media might induce untangling of physical cross-linking, such as entanglements, followed by a decrease in cross-linking density during swelling. In contrast, the swelling of the ATRP networks does not affect their cross-linking density because of the homogeneously cross-linked structure (Fig. 2), which is the number of cross-links per polymer volume fraction. In addition, FRP gels with cross-linker content of less than 5 mol% show little changes in the cross-linking density, whereas those with more than 5 mol% decreased the cross-linking density because of swelling, implying that the ATRP gels have fewer inhomogeneous structures and that the network structures of the FRP gels become more inhomogeneous as the cross-linker content increases.

Temperature-responsive properties

Several PNIPAAm-based gels have been designed as temperature-responsive gels. We previously reported the temperature-responsive properties of PNIPAAm gels synthesized via ATRP and FRP with cross-linker content of 3 mol% at 5 °C and 25 °C.[43] ATRP and FRP gels synthesized at 5 °C showed temperature-responsive shrinkage at 32 °C, which is the lower critical solution temperature (LCST) of PNIPAAm. However, while the temperature-responsiveness of the FRP gel synthesized at 25 °C was
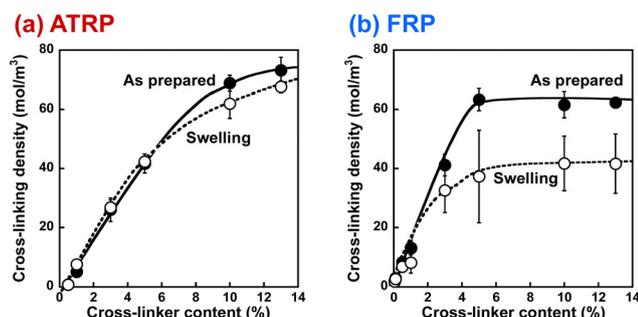

Fig. 1 The effect of the cross-linker content on the cross-linking density of the PNIPAAm gels (●, as-prepared; ○, swollen) synthesized via ATRP (a) and FRP (b). The cross-linking densities were determined from the compression modulus.
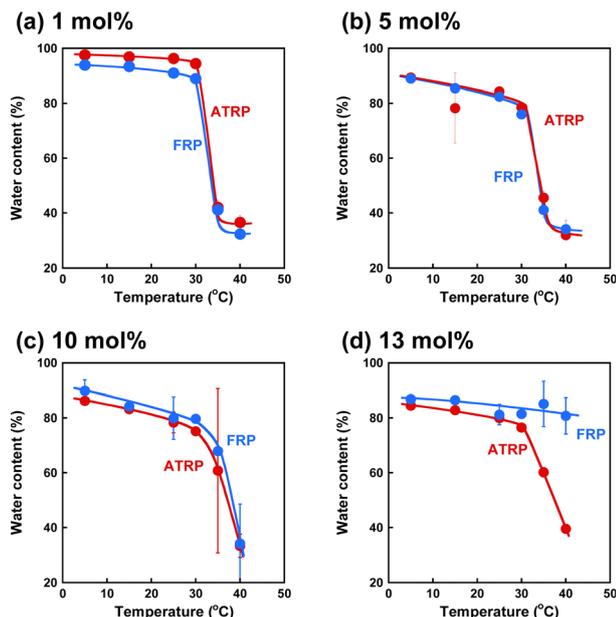
Fig. 3 The relationship between temperature and water content of PNI-PAAm gels with various cross-linker contents synthesized *via* ATRP (red) and FRP (blue) at 5 °C.

likely to disappear, that of the ATRP gel remained. The previous study compared the temperature-responsive properties of ATRP and FRP gels synthesized with cross-linker content of 3 mol% from the viewpoint of their network structures. Generally, the network structures of gels are directly correlated with the cross-linker content and affect their properties and functions. In this study, we investigated the temperature-responsive properties of ATRP and FRP gels synthesized with various cross-linker contents at 5 °C.

Fig. 3 shows the effect of temperature on the water content of the ATRP and FRP gels synthesized with various cross-linkers at 5 °C. Similar to the ATRP and FRP gels with cross-linker content of 3 mol% reported previously,[43] ATRP and FRP gels with cross-linker content of less than 10 mol% exhibited a drastic decrease in the water content with increasing temperatures above 32 °C. In contrast, while the water content of the ATRP gel with cross-linker content of 13 mol% decreased dramatically above 32 °C, the FRP gel did not. In a previous paper,[43] we reported that the temperature-responsiveness of ATRP gel synthesized with cross-linker content of 3 mol% at 25 °C exhibited temperature-responsive but that of the FRP gel synthesized at 25 °C disappeared because of their inhomogeneous structures. Although FRP at 25 °C formed a more inhomogeneous network structure of the PNIPAAm gel than that at 5 °C, ATRP synthesized at 5 °C and 25 °C formed a more homogeneous structure. Unlike the previous paper, this paper focuses on the effect of cross-linker content on the network structures and temperature-responsiveness of ATRP and FRP gels synthesized at 5 °C. Interestingly, the temperature-responsiveness of the FRP gel with cross-linker content of 13 mol% disappeared despite the polymerization at 5 °C, implying that the polymerization with high cross-linker content formed inhomogeneous networks, similar to the polymerization at a

temperature near LCST of PNIPAAm. Shibayama *et al.* reported that the phase-transition temperature of FRP-prepared PNIPAAm gels was independent of the cross-linker content, although an increase in the cross-linker content induced a decrease in the swelling ratio in the swollen state.[49] Specifically, the PNIPAAm gel with low cross-linker content shrinks more sharply than the gel with high cross-linker content. Shibayama's results support our finding that the temperature-responsiveness of FRP gels with cross-linker content of 13 mol% is decreased. Note that ATRP gels with high cross-linker content of 13 mol% showed a drastic decrease in water content at 32 °C, similar to ATRP and FRP gels with low cross-linker content. The temperature-responsiveness of the PNIPAAm gels is strongly influenced by the inhomogeneity of their networks. The difference in the temperature-responsive behavior between the ATRP and FRP gels with a cross-linker content of 13 mol% might suggest that ATRP enables us to form a more homogeneous network even though the polymerization is performed with high cross-linker contents, unlike FRP. In this study, therefore, we investigated the effect of the cross-linker content and temperature on the network structure of the ATRP and FRP gels quantitatively, as mentioned in the following sections.

The effect of cross-linker content on network structures of ATRP gels

Generally, polymer gels are difficult to characterize their structures because they have chemically cross-linked networks and are not dissolved in any solvent. However, DLS is a powerful tool for characterizing the 3D network structures of polymer gels. For example, DLS measurements have been used to evaluate the inhomogeneity and correlation length of polymer networks. In this study, we used DLS measurements to compare the network structures of ATRP and FRP gels with different cross-linker contents. In the DLS measurements, the time average scattered intensity, $\langle I \rangle_T$, was measured at 100 different sample positions of their gels. The apparent diffusion coefficient, D_A, at each sample position was also determined from the correlation function using the partial heterodyne method.[34–40] The intensity correlation functions for the ATRP and FRP gels at an arbitrary position exhibited similar decay profiles, meaning that they can be fitted by the similar equation (Fig. S1, ESI†). D and the dynamic fluctuations, $\langle I \rangle_F$, were obtained from the slope and intercept in the linear relationship between $\langle I \rangle_T / D_A$ and $\langle I \rangle_T$ for the gel (Fig. S2, ESI†). Furthermore, the correlation lengths, ξ, of the networks were determined from D using eqn (10). The effects of the cross-linker content on $\langle I \rangle_F$, $\langle I \rangle_C$, and ξ of the ATRP and FRP gels at 25 °C, which is a temperature below LCST of PNIPAAm, are shown in Fig. 4. The data reported in our previous study[43] are replotted as ξ of both ATRP and FRP gels with cross-linker content of 3 mol% (Fig. 4). The total intensity of scattered light from polymer gels is based on two contributions, namely, scattering from the dynamic concentration fluctuations (liquid-like contribution), $\langle I \rangle_F$, and scattering from the spatial inhomogeneity (solid-like contribution), $\langle I \rangle_C$, as represented by eqn (1). The static component derived from spatial fluctuation is introduced during the formation of
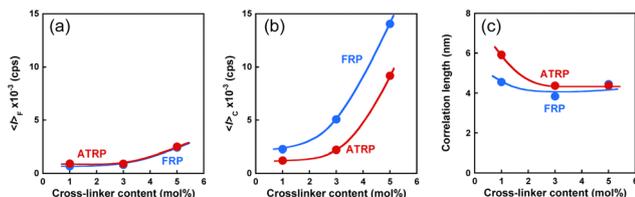
Fig. 4 The effect of the cross-linker content on (a) $\langle I \rangle_F$, (b) $\langle I \rangle_C$, and (c) ξ of the ATRP and FRP gels at 25 °C. Their gels were synthesized with various cross-linker content at 5 °C.

the three-dimensional polymer networks.[37,38] The topological constraints during the network formation result in static frozen inhomogeneities depending on the preparation temperature and the degree of cross-links. The $\langle I \rangle_C$ of ATRP and FRP gels is much greater than that of $\langle I \rangle_F$ (Fig. 4(a) and (b)), implying that $\langle I \rangle_T$ is more predominantly governed by $\langle I \rangle_C$ than by $\langle I \rangle_F$. Therefore, the high light-scattered intensity of the ATRP and FRP gels is mainly caused by spatial inhomogeneity. An increase in the cross-linker content resulted in a slight increase in $\langle I \rangle_F$ and a drastic increase in $\langle I \rangle_C$ of the ATRP and FRP gels. $\langle I \rangle_F$ is not influenced by cross-linker content because it is based on the dynamic fluctuation of the polymer chains. However, the drastic increase in $\langle I \rangle_C$ of the ATRP and FRP gels indicates that increasing the cross-linker content enhances the inhomogeneity of the gel networks. Although there is no difference in $\langle I \rangle_F$ between the ATRP and FRP gels, $\langle I \rangle_C$ of the ATRP gel is lower than that of the FRP gel, implying that the former gel has fewer inhomogeneous networks than the latter. With increasing the cross-linker content, ξ of the ATRP and FRP gels trended to decrease. This indicates that the mesh sizes of their networks decrease with increasing cross-linker content. As eqn (10) means that D is inversely proportional to ξ, the decrease in ξ of both gels with increasing cross-linker content is attributed to an increase in their collective diffusion coefficient. While ξ of the ATRP gel with cross-linker content of less than 3 mol% is greater than that of the FRP gel, their gels with cross-linker content of more than 3 mol% showed no significant difference in the ξ. The variation of scattered intensity was directly and quantitatively evaluated as no clear difference in the network structure between ATRP and FRP gels with various cross-linker contents was found in ξ.

Norisuye *et al.* previously compared the network structure of polymer gels prepared by FRP and γ-ray irradiation method using the average of $\langle I \rangle_T$.[39] FRP polymer gels exhibited greater $\langle I \rangle_T$ than those by the γ-ray irradiation method. Their studies reported that FRP formed inhomogeneous networks because of the formation of cross-linking clusters. The $\langle I \rangle_F$ from polymer gels is very small because it is based on the concentration fluctuations of polymer chains with high mobility (Fig. 4(a) and (b)). However, as $\langle I \rangle_C$ is based on spatial inhomogeneity, such as the inhomogeneity of the distribution of cross-links, it strongly depends on the sample position. This means that the variation in $\langle I \rangle_T$ is mainly governed by that of $\langle I \rangle_C$. Therefore, the inhomogeneity of the networks can be evaluated from the variation in $\langle I \rangle_T$ of the polymer gels. For example, ATRP and FRP gels have distributions

in $\langle I \rangle_T$, as shown from the histograms of the number of $\langle I \rangle_T$ in Fig. S3 (ESI†), implying that their gels have spatial inhomogeneity in their networks. The distribution of $\langle I \rangle_T$ for the ATRP gel is narrower than that for the FRP gel. We determined the standard deviations of $\langle I \rangle_T$ for ATRP and FRP gels to compare their network inhomogeneity quantitatively. The relationship between the cross-linker content and standard deviation for distributing $\langle I \rangle_T$ for ATRP and FRP gels with cross-linker content of 3 mol% at 25 °C is shown in Fig. 5. The standard deviation of $\langle I \rangle_T$ for both gels increased gradually as cross-linker content increased. A large standard deviation shows that $\langle I \rangle_T$ has a wide distribution depending on the sample position. The increase in the standard deviation shows that increasing cross-linker content makes the gel networks more inhomogeneous.[26,34,37] Interestingly, the standard deviation of $\langle I \rangle_T$ for the ATRP gel with several cross-linker contents is much smaller than that for the FRP gel. When the cross-linker content was increased up to 5 mol%, the standard deviation of $\langle I \rangle_T$ increased drastically in the FRP gel but only slightly in the ATRP gel. Particularly, the standard deviation of $\langle I \rangle_T$ for the ATRP gel with cross-linker content of 5 mol% was one-third smaller than that for the FRP gel with the same cross-linker content. The smaller standard deviation of $\langle I \rangle_T$ for the ATRP gel than the FRP gel quantitatively indicates that the former gel had a more homogeneous network than the latter gel (Fig. 6). We conclude that ATRP is more effective than FRP at reducing the spatial inhomogeneity of gel networks, *i.e.*, the inhomogeneity of the distribution of cross-links. The standard deviation clarifies that the networks of the ATRP and FRP gels with a cross-linker content of 5 mol% or less have different inhomogeneities although they exhibited similar temperature-responsive behavior. Importantly, this study reports that a standard deviation of $\langle I \rangle_T$ for polymer gels is a useful indicator to quantitatively evaluate the inhomogeneity of the polymer networks.

The effect of temperature on network structures of ATRP gels

The ATRP and FRP gel change their water content in response to temperature changes, as previously described. Their gels swell in the water below 32 °C but shrink above 32 °C. Therefore, their
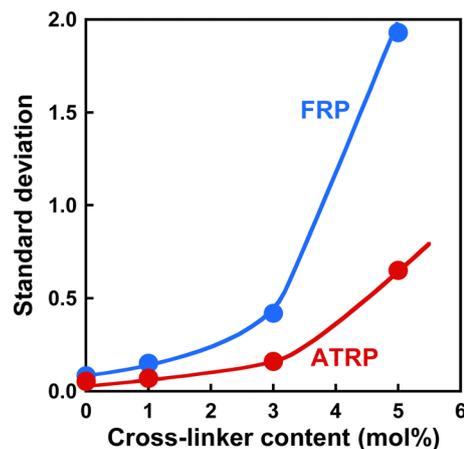

Fig. 5 The effect of the cross-linker content on the standard deviation of $\langle I \rangle_T$ for the ATRP (red) and FRP (blue) gels at 25 °C.
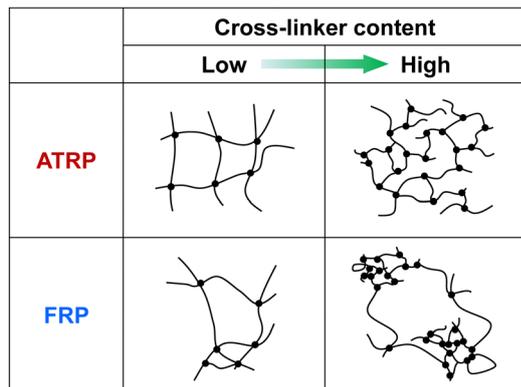
Fig. 6 Tentative illustration for inhomogeneity of ATRP and FRP gels with low and high cross-linker content.

network structures strongly depend on temperature. Unfortunately, the ATRP and FRP gels become turbid above 32 °C, making DLS evaluation difficult. However, as an increase in temperature below 32 °C induces a small change in the conformation of polymer chains because of the high-temperature sensitivity of PNIPAAm chains, the change in the network structures of the ATRP and FRP gels according to a temperature change below 32 °C must be investigated. The effect of temperature on $\langle I \rangle_F$, $\langle I \rangle_C$, and ξ of the ATRP and FRP gels. $\langle I \rangle_F$ of both ATRP and FRP gels increase slightly with rising temperature (Fig. 7). Rising temperature increases the mobility of polymer chains, which is followed by a slight increase in dynamic fluctuations. There is little difference in $\langle I \rangle_F$ between the ATRP and FRP gels because the dynamic fluctuation based on the mobility of the polymer chains of the ATRP gel is almost the same as that of the FRP gel. However, $\langle I \rangle_C$ of both gels was much greater than $\langle I \rangle_F$, indicating that the scattered intensity of their gels is more strongly governed by spatial fluctuation than by dynamic fluctuation. Notably, $\langle I \rangle_C$ of the ATRP gel was smaller than that of the FRP gel, implying that ATRP gels have smaller spatial fluctuation than FRP gels. In addition, while $\langle I \rangle_C$ of the FRP gel increased sharply as temperature increased, an increase in $\langle I \rangle_C$ of the ATRP is effectively suppressed at temperatures less than 30 °C. Even when temperature increased near LCST of PNIPAAm, $\langle I \rangle_C$ of the ATRP gel was suppressed to half of the FRP gel. Increasing temperature amplifies the spatial fluctuation of ATRP and FRP gels because their PNIPAAm chains shrink owing to a change from hydrophilic to hydrophobic. However, the more homogeneous structure of the ATRP gel suppresses the amplification of the spatial fluctuation of the networks unlike that of the FRP gel. In addition, ξ of the ATRP

and FRP gels increased with increasing temperature. Shibayama *et al.* described that ξ of polymer gels is not the real mesh size of the network but correspond to concentration fluctuations.[26] Their study reported that ξ of temperature-responsive polymer gels increased with increasing temperature and diverged to infinity at the LCST. The increase in ξ of the ATRP and FRP gels agrees with the previous study by Shibayama *et al.* As eqn (10) means that D is inversely proportional to ξ, the increase in ξ of both gels indicates that their collective diffusion coefficient decreases with increasing temperature. There was no difference in ξ between the ATRP and FRP gels because both gels show the same temperature-responsive behavior.

To investigate the effect of temperature on the inhomogeneity of ATRP and FRP gels, we determined the standard deviation of their $\langle I \rangle_T$ as a function of temperature. The relationship between temperature and standard deviation of $\langle I \rangle_T$ for ATRP and FRP gels is shown in Fig. 8. While the standard deviation of $\langle I \rangle_T$ for FRP gels increased sharply with increasing temperatures near LCST of PNIPAAm, that for ATRP gel remains constant at temperatures below 32 °C and increased slightly at 32 °C. Note that the standard deviation of $\langle I \rangle_T$ for the ATRP gel was smaller than that for the FRP gel in various temperatures. The small standard deviation of $\langle I \rangle_T$ implies that the ATRP gel has a more homogeneous network than the FRP gel. In addition, the standard deviation for the ATRP gel implies that the enhancement of the inhomogeneity caused by rising temperature is more effectively suppressed in the ATRP gel than in the FRP gel. Our previous study discussed the different inhomogeneities of the PNIPAAm gel networks from the viewpoint of the polymerization mechanisms of ATRP and FRP as follows.[43] In the intermediate stage of polymerization, finite clusters formed by ATRP have a lower cross-linked structure than those by FRP. During the gelation stage, although FRP induces the formation of infinite clusters in which highly cross-linked nanodomains are inhomogeneously distributed, ATRP enables the formation of infinite clusters with relatively homogeneous networks. In addition to the results reported in our previous study, we demonstrated the
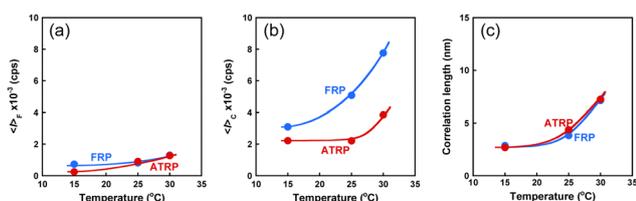

Fig. 7 Effect of temperature on (a) $\langle I \rangle_F$, (b) $\langle I \rangle_C$, and (c) ξ of the ATRP and FRP gels at 25 °C. These gels were synthesized with a cross-linker content of 3 mol% at 5 °C.
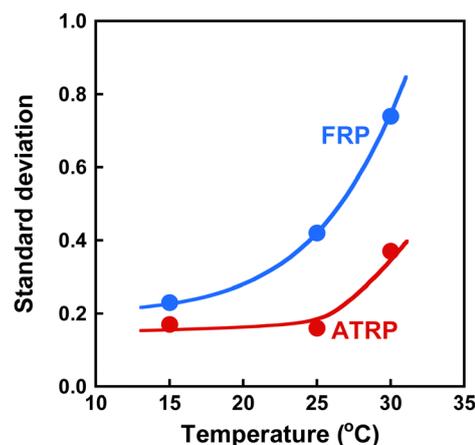

Fig. 8 The effect of the temperature on the standard deviation of $\langle I \rangle_T$ for the ATRP (red) and FRP (blue) gels. These gels were synthesized with a cross-linker content of 3 mol% at 25 °C.

quantitative evaluation of the inhomogeneity of ATRP and FRP gels using light scattered intensity and standard deviation in this study. These results indicate that the standard deviation of the scattered intensity is a useful indicator for quantitatively evaluating the network inhomogeneity because the scattered intensity of polymer gels with inhomogeneous structures depends strongly on the sample position. The quantitative evaluation of the inhomogeneity using standard deviation demonstrates that ATRP enables the formation of more homogeneous networks than FRP.

Conclusions

In this study, we used DLS measurements to investigate the network structure of PNIPAAm gels synthesized *via* ATRP and FRP. The FRP gel with high cross-linker content showed no temperature-responsiveness, whereas the ATRP gel shrank drastically in response to temperature despite the high cross-linker content. The dynamic fluctuation, $\langle I \rangle_\mathrm{F}$, and spatial inhomogeneity, $\langle I \rangle_\mathrm{C}$, contributing to the light-scattered intensity and correlation length, ξ, of the ATRP and FRP gels were determined as a function of the cross-linker content and temperature. The $\langle I \rangle_\mathrm{C}$ of both the ATRP and FRP gels was much greater than $\langle I \rangle_\mathrm{F}$, revealing that their gels have spatial inhomogeneities. The ξ of both the ATRP and FRP gels increased as the cross-linker content and temperature increased, but there was no difference between their gels. While there was no difference in $\langle I \rangle_\mathrm{F}$ between the ATRP and FRP gels, $\langle I \rangle_\mathrm{C}$ of the ATRP gels was smaller than that of the FRP gels. Increasing the temperature caused a significant increase in $\langle I \rangle_\mathrm{C}$ of the FRP gel but only a slight increase in $\langle I \rangle_\mathrm{C}$ of the ATRP gel. The small $\langle I \rangle_\mathrm{C}$ of the ATRP gels shows that the ATRP gels have more homogeneous networks than the FRP gels. In addition, we proposed a new method for quantifying the inhomogeneity of gel networks, using the standard deviation of the scattered intensity of polymer gels. The standard deviation of scattered intensity of ATRP gels became much smaller than that of FRP gels with any cross-linker content. Although the standard deviation of $\langle I \rangle_\mathrm{T}$ for the FRP gels increased sharply with temperature, ATRP gels do not. Therefore, we conclude that ATRP enables the formation of a more homogeneous network than FRP. Even though further research into the effects of the homogeneity on the mechanical and responsive properties of the ATRP gels is required, quantitative evaluations of the inhomogeneity of the network structures by the standard deviation of the scattered intensity will be useful in the investigation of the structure–property relationships of gels.

Conflicts of interest

There are no conflicts to declare.

Acknowledgements

References

1 A. S. Hoffman, Hydrogels for biomedical applications, *Adv. Drug Delivery Rev.*, 2002, **54**, 3–12.

2 T. Miyata, T. Uragami and K. Nakamae, Biomolecule-sensitive hydrogels, *Adv. Drug Delivery Rev.*, 2002, **54**, 79–98.

3 Z. M. O. Rzaev, S. Dinçer and E. Pişkin, Functional copolymers of *N*-isopropylacrylamide for bioengineering applications, *Prog. Polym. Sci.*, 2007, **32**, 534–595.

4 T. Miyata, Preparation of smart soft materials using molecular complexes, *Polym. J.*, 2010, **42**, 277–289.

5 T. Miyata, N. Asami and T. Uragami, A reversibly antigen-responsive hydrogel, *Nature*, 1999, **399**, 766–769.

6 J. S. Mohammed and W. L. Murphy, Bioinspired Design of Dynamic Materials, *Adv. Mater.*, 2009, **21**, 2361–2374.

7 M. A. Cohen Stuart, W. T. S. Huck, J. Genzer, M. Müller, C. Ober, M. Stamm, G. B. Sukhorukov, I. Szleifer, V. V. Tsukruk, M. Urban, F. Winnik, S. Zauscher, I. Luzinov and S. Minko, emerging applications of stimuli-responsive polymer materials, *Nat. Mater.*, 2010, **9**, 101–113.

8 Y. Qiu and K. Park, Environment-sensitive hydrogels for drug delivery, *Adv. Drug Delivery Rev.*, 2012, **64**, 49–60.

9 M. Wei, Y. Gao, X. Li and M. J. Serpe, Stimuli-responsive polymers and their applications, *Polym. Chem.*, 2017, **8**, 127–143.

10 H. R. Culver, J. R. Clegg and N. A. Peppas, Analyte-Responsive Hydrogels: Intelligent Materials for Biosensing and Drug Delivery, *Acc. Chem. Res.*, 2017, **50**, 170–178.

11 M. Vazquez-Gonzalez and I. Willner, Stimuli-responsive biomolecule-based hydrogels and their applications, *Angew. Chem., Int. Ed.*, 2020, **59**, 15342–15377.

12 X. Liu, J. Liu, S. Lin and X. Zhao, Hydrogel machines, *Mater. Today*, 2020, **36**, 102–124.

13 P. Sikdar, M. M. Uddin, T. M. Dip, S. Islam, M. S. Hoque, A. K. Dhare and S. Wu, Recent advances in the synthesis of smart hydrogels, *Mater. Adv.*, 2021, **2**, 4532–4573.

14 K. Zhang, Q. Feng, Z. Fang, L. Gu and L. Bian, Structurally dynamic hydrogels for biomedical applications: pursuing a fine balance between macroscopic stability and microscopic dynamics, *Chem. Rev.*, 2021, **121**, 11149–11193.

15 Y. Okumura and K. Ito, The polyrotaxane gel: a topological gel by figure-of-eight cross-links, *Adv. Mater.*, 2001, **13**, 485–487.

16 Y. Noda, Y. Hayashi and K. Ito, From topological gels to slide-ring materials, *J. Appl. Polym. Sci.*, 2014, **131**, 40509.

17 K. Haraguchi and T. Takehisa, Nanocomposite hydrogels: a unique organic–inorganic network structure with extraordinary mechanical, optical, and swelling/de-swelling properties, *Adv. Mater.*, 2002, **14**, 1120–1124.

18 J. P. Gong, Y. Katsuyama, T. Kurokawa and Y. Osada, Double-network hydrogels with extremely high mechanical strength, *Adv. Mater.*, 2003, **15**, 1155–1158.

19 J. P. Gong, Why are double network hydrogels so tough?, *Soft Matter*, 2010, **6**, 2583–2590.

20 T. Nakajima, Generalization of the sacrificial bond principle for gel and elastomer toughening, *Polym. J.*, 2017, **49**, 447–485.

21 C. Norioka, Y. Inamoto, C. Hajime, A. Kawamura and T. Miyata, A universal method to easily design tough and stretchable hydrogels, *NPG Asia Mater.*, 2021, **13**, 34.

22 R. Yoshida, K. Uchida, Y. Kaneko, K. Sakai, A. Kikuchi, Y. Sakurai and T. Okano, Comb-type grafted hydrogels with rapid deswelling response to temperature changes, *Nature*, 1995, **374**, 240–242.

23 E. C. Cho, J. W. Kim, A. Fernandez-Nieves and D. A. Weitz, Highly responsive hydrogel scaffolds formed by three-dimensional organization of microgel nanoparticles, *Nano Lett.*, 2008, **8**, 168–172.

24 N. Morimoto, T. Ohki, K. Kurita and K. Akiyoshi, Thermo-Responsive hydrogels with nanodomains: rapid shrinking of a nanogel-crosslinking hydrogel of poly(N-isopropyl acrylamide), *Macromol. Rapid Commun.*, 2008, **29**, 672–676.

25 J. A. Yoon, T. Kowalewski and K. Matyjaszewski, Comparison of thermoresponsive deswelling kinetics of poly(oligo(ethylene oxide) methacrylate)-based thermoresponsive hydrogels prepared by "graft-from" ATRP, *Macromolecules*, 2011, **44**, 2261–2268.

26 M. Shibayama, Universality and specificity of polymer gels viewed by scattering methods, *Bull. Chem. Soc. Jpn.*, 2006, **79**, 1799–1819.

27 M. Shibayama, Small-angle neutron scattering on polymer gels: phase behavior, inhomogeneities and deformation mechanisms, *Polym. J.*, 2010, **43**, 18–34.

28 M. Shibayama, Structure-mechanical property relationship of tough hydrogels, *Soft Matter*, 2012, **8**, 8030–8038.

29 T. Matsunaga, T. Sakai and Y. Akagi, U.-i. Chung and M. Shibayama, Structure characterization of tetra-PEG gel by small-angle neutron scattering, *Macromolecules*, 2009, **42**, 1344–1351.

30 T. Sakai, Y. Akagi, T. Matsunaga, M. Kurakazu, U. I. Chung and M. Shibayama, Highly elastic and deformable hydrogel formed from tetra-arm polymers, *Macromol. Rapid Commun.*, 2010, **31**, 1954–1959.

31 K. Nishi, M. Chijiishi, Y. Katsumoto, T. Nakao, K. Fujii, U. I. Chung, H. Noguchi, T. Sakai and M. Shibayama, Rubber elasticity for incomplete polymer networks, *J. Chem. Phys.*, 2012, **137**, 224903.

32 S. Kondo, H. Sakurai, U.-I. Chung and T. Sakai, Mechanical properties of polymer gels with bimodal distribution in strand length, *Macromolecules*, 2013, **46**, 7027–7033.

33 P. N. Pusey and W. Van Megen, Dynamic light scattering by non-erogodic media, *Phys. A*, 1989, **157**, 705–741.

34 M. Shibayama, T. Norisuye and S. Nomura, Cross-link density dependence of spatial inhomogeneities and dynamic fluctuations of poly(N-isopropylacrylamide) gels, *Macromolecules*, 1996, **29**, 8746–8750.

35 M. Shibayama, Y. Fujikawa and S. Nomura, Dynamic light scattering study of poly(N-isopropylacrylamide-co-acrylic acid) gels, *Macromolecules*, 1996, **29**, 6535–6540.

36 M. Shibayama, F. Ikkai, Y. Shiwa and Y. Rabin, Effect of degree of cross-linking on spatial inhomogeneity in charged gels. I. Theoretical predictions and light scattering study, *J. Chem. Phys.*, 1997, **107**, 5227–5235.

37 M. Shibayama, Spatial inhomogeneity and dynamic fluctuations of polymer gels, *Macromol. Chem. Phys.*, 1998, **199**, 1–30.

38 M. Shibayama, S.-i Takata and T. Norisuye, Static inhomogeneities and dynamic fluctuations of temperature sensitive polymer gels, *Phys. A*, 1998, **249**, 245–252.

39 T. Norisuye, Y. Kida, N. Masui, Q. Tran-Cong-Miyata, Y. Maekawa, M. Yoshida and M. Shibayama, Studies on two types of built-in inhomogeneities for polymer gels: frozen segmental concentration fluctuations and spatial distribution of cross-Links, *Macromolecules*, 2003, **36**, 6202–6212.

40 T. Norisuye, Q. Tran-Cong-Miyata and M. Shibayama, Dynamic inhomogeneities in polymer gels investigated by dynamic light scattering, *Macromolecules*, 2004, **37**, 2944–2953.

41 E. Geissler and A. M. Hecht, Rayleigh light scattering from concentrated solutions of polystyrene in cyclohexane, *J. Chem. Phys.*, 1976, **65**, 103–110.

42 E. Geissler and A. M. Hecht, Dynamic light-scattering from polyacrylamide-water gels, *J. Phys.*, 1978, **39**, 955–960.

43 C. Norioka, A. Kawamura and T. Miyata, Mechanical and responsive properties of temperature-responsive gels prepared via atom transfer radical polymerization, *Polym. Chem.*, 2017, **8**, 6050–6057.

44 Q. Liu, P. Zhang, A. Qing, Y. Lan and M. Lu, Poly(N-isopropylacrylamide) hydrogels with improved shrinking kinetics by RAFT polymerization, *Polymer*, 2006, **47**, 2330–2336.

45 T. Masuda and M. Takai, Structure and properties of thermoresponsive gels formed by RAFT polymerization: effect of the RAFT agent content, *Polym. J.*, 2020, **52**, 1407–1412.

46 T. Miyata, A. Jikihara, K. Nakamae and A. S. Hoffman, Preparation of poly(glucosyloxyethyl methacrylate)-concanavalin A complex hydrogel and its glucose-sensitivity, *Macromol. Chem. Phys.*, 1996, **197**, 1135–1146.

47 T. Miyata, M. Jige, T. Nakaminami and T. Uragami, Tumor marker-responsive behavior of gels prepared by biomolecular imprinting, *Proc. Natl. Acad. Sci. U. S. A.*, 2006, **103**, 1190–1193.

48 J. G. H. Joosten, J. L. McCarthy and P. N. Pusey, Dynamic and static light scattering by aqueous polyacrylamide gels, *Macromolecules*, 1991, **24**, 6690–6699.

49 M. Shibayama, Y. Shirotani, H. Hirose and S. Nomura, Simple scaling rules on swollen and shrunken polymer gels, *Macromolecules*, 1997, **30**, 7307–7312.